



## **GEOTECHNICAL SITE INVESTIGATION OF SUBSURFACES BY SURFACE WAVES CONSIDERING HIGHER MODES**

**Frank WUTTKE<sup>1</sup>, Hans-Gottfried SCHMIDT<sup>2</sup>, Tom SCHANZ<sup>3</sup>**

### **SUMMARY**

The analysis of seismic affected areas and the evaluation of seismic risk of the developed areas demand the knowledge of the dynamic site characterisation. While doing so, the site dependent seismic excitation including the dominant site frequencies and the filtering and amplification effects are necessary to be determined. Beside the earthquake characteristics, the realistic soil parameters are also needed for the numerical site investigations. Undisturbed soil profiles can be efficiently assessed with the help of the surface wave propagation. By using inversion methods, the soil stiffness profiles can then be calculated. In such cases, mostly the measured fundamental mode of the surface wave is used without the consideration of higher modes of surface waves. However for describing the complete surface wave propagation, all the excited modes are necessary. In this paper, the appeared higher modes of the surface waves were detected by using various multi-trace methods. Also, an inversion method was used that considers various higher modes. Some field measurement data were utilised to determine the dispersion characteristics using the inversion method. While considering the higher modes, the weighted excitation factors were used. In this way, the realistic soil shear wave profiles were obtained. The shear wave profiles can be utilised to calculate stiffness profiles.

### **INTRODUCTION**

Seismic methods are used to explore soil profiles in a non-destructive way. The seismic methods provide soil parameters for static and as well as for dynamic calculations. In the static case, the seismic methods provide the small strain parameter for the description of more realistic stress- and strain-dependent soil parameters. For the examination of natural geological sites and reclaimed mining areas, the surface waves was used to provide the soil profile and stiffness parameters for the small strain level. The small strain parameters are later used to determine foundation settlements.

---

<sup>1</sup> Research student, <sup>2</sup> Reseach Assistant & <sup>3</sup> Professor, Laboratory of Soil Mechanics, Bauhaus-University Weimar, Faculty of Civil Engineering, 99423 Weimar, Germany. Tel: 0049-3643-584554, Fax: 0049-3643-584564, [www.uni-weimar.de/geotechnik](http://www.uni-weimar.de/geotechnik)

The surface waves possess a pronounced sensitivity for the existing shear wave speeds in a soil profile and do not react so sensitively to water table within the layered halfspace as compared to other seismic methods. Therefore, the surface waves are usually determined. To consider as far as possible all information of the surface wave field, it is desirable that they should include all the appeared modes. To achieve this goal two essential parts are necessary: (a) a method for analysing dispersion characteristics and separate the different modes, and (b) an inversion procedure to consider all the appeared modes and determine the soil profiles.

Various methods exists to determine the dispersion characteristics in soils. Very often the procedure of spectral analysis of surface waves (SASW) has been used in field of geotechnics. The SASW method uses the phase differences between two receivers for the determination of the dispersion characteristics. The drawback of this method is the calculation of only one dispersion curve for the entire dispersion characteristics of the soil. A detection of different excited modes is not possible with this method. However, it is well known by now that the higher modes contribute important information of the dispersion characteristics if some of them are excited.

To visualise separate excited modes in the measured surface wave field several multi-trace method were used in this paper. These methods were tested for their usability. The advantages and disadvantages of the commonly used methods are discussed to obtain correct information about the wave dispersion. To obtain the soil profile the iterative Levenberg-Marquardt procedure was modified so that all detected modes can be inverted.

## THEORETICAL BACKGROUND OF THE DISPERSION ANALYSES

Several approaches have been suggested in the past to determine the dispersion characteristics in soils. Equation (1) and (2) have been proposed by [1] and [3], respectively. Equation (1) is the well known frequency wave number analysis (f – k analysis) [1] for plane waves.

$$S(\omega, k) = \int_{-\infty}^{\infty} \int_{-\infty}^{\infty} u(t, x) e^{-i(\omega t + 2pkx)} dt dx \quad (1)$$

$$S(\omega, p) = \int_{-\infty}^{\infty} \left\{ \sum_{j=1}^n u(x_j, \tau + px_j) V_{x_j} \right\} e^{-i\omega\tau} d\tau \quad \text{with } j \in \mathbf{N} \quad (2)$$

For the calculation of images by using the f-k analysis the existing rules to avoid aliasing signals have been considered [1]. The wave field transformation as suggested by [6] offers an improved possibility in the representation of the dispersion characteristics. A time-shifted stacking of the seismogram to different offsets has been implemented, whereby the wave field is divided into its even slowness parameters  $p$  ( $p = 1/c$ ). After the stacking procedure a one dimensional fourier transform by considering the intercept time,  $\tau$ , is executed. The final result of the transform are the image of the wave field in the slowness - frequency domain ( $\omega$ - $p$  domain).

Alternative to the wave field transformation for a plane wave propagation, a discrete Bessel transformation for a rotationally symmetric wave propagation can be used [3]. The existing Bessel function is replaced thereby with the appropriate Hankel functions. If we use the Hankel function for a

outgoing wavefield within the transformation as suggested by [3], the frequency lowness spectrum results to the following expression:

$$S(\omega, p) \approx \sum_{j=1}^M u(\omega, r_j) H_0^2(\omega p r_j) r_j \Delta r_j \quad \text{with } j \in \mathbb{N} \quad (3)$$

According to equation (3), the discrete Bessel transformation represents a special type of wave field transformation. In the evaluation of the spectra, the existing rules are to be considered for the appearance of a spatial aliasing. According to [9], the first aliasing signal for the wave field transformation can be indicated as:  $p_n = p_{ref} - n(f \Delta x)^{-1}$  with  $n \in \mathbb{Z}$ . The accuracy of the determined dispersion curves, which were computed on the basis of measurements with relatively short offset length was improved when used together with the aforementioned methods [8]. Equation (4) is proposed by [8]. In Equation (4), the influence of the amplitudes is neglected within the complex spectra and only the phase that is related to the dispersion characteristics is considered. The conversion is the simplest, if the individual traces are transformed into the frequency domain before the summation over the offset took place.

$$S(\omega, \phi) = \int_{-\infty}^{\infty} e^{i\phi x} [U(x, \omega) / |U(x, \omega)|] dx \quad (4)$$

For studying the properties of wave propagations and the efficiency of the proposed methods the calculation of synthetic wave field is necessary. One possibility is to use the normal mode superposition because the body wave do not supply an appreciable contribution to the analysed field in a greater distance from the source. To study the behavior of separate wave types during the propagation in vertical heterogenous media, the solution of a excited layered halfspace were carried out by means of the contour integration and the residual theorem. For the study of the surface waves, it is sufficient to use the part of the solution which corresponds to the residual term. The used part is identical to the Green's function of surface waves in the frequency domain. By taking an inverse Fourier transform as shown in Equation (5), the solution is transformed back in the original time domain. In numerical solution, the inverse Fourier transform were executed as the Inverse Fast Fourier Transform.

$$u_z(t, r) = i \frac{F_z}{2} \int_0^{\infty} \sum_{\kappa=1}^n \text{Re} s \left\{ u_z^{H_0}(\mu, c_s, c_p, z, k, \omega) k H_0^2(kr) \right\} \Big|_{k=\kappa_n} e^{i\omega t} d\omega \quad \text{with } n \in \mathbb{N}, n \neq 0 \quad (5)$$

In Equation (5), the expression  $u_z^{H_0}(\mu, c_s, c_p, z, k, \omega)$  represents the vertical displacement on the surface of a layered half space in terms of reflection and transmission coefficients. The calculation of the displacement taking place by wave numbers corresponds to the eigenvalues,  $\kappa_n$ , on the given frequency  $\omega$  ( $n$  is the number of eigenvalues to a given frequency). The upper subscript  $H_0$  represents the used type of Hankel function in the Hankel transform for the solution of partial differential equation and is important for the back transform process in the space domain. The basis for the coupling of the existing layers is the generalized reflection and transmission coefficient method as suggested by [2] and [4]. During the investigation only the vertical displacement components which can be measured due to a vertical impulse point load on the halfspace surface were considered. To obtain the resulting synthetic seismogram a convolution between the Green's function and a Ricker impulse of 3<sup>rd</sup> order (as signal for the sledge hammer or a drop weight excitation) were considered. The computed distances of the geophones chosen were similar to the expected experimental offsets during the measurements.

At first, the contemplation of the dispersion characteristics is presented via an example. To evaluate the performance of Equation (1), (2) and (3), following soil profile was used:  $c_s = (400, 1000)$  [m/s],  $c_p = (700, 1700)$  [m/s],  $\rho = (1.7, 2.0)$  [g/cm<sup>3</sup>],  $h = 10$  [m];  $c_s$  and  $c_p$  are the shear and the longitudinal wave velocities, respectively,  $\rho =$  density,  $h =$  layer thickness. The values within the brackets are the first layer and the second values represent the halfspace.

Figure 1(a) shows the synthetic wave field generated by using Equation (5). Figure 1(b) and 1(c) present the phase velocity spectra and wave number spectra obtained by using Equation (2) and (1), respectively. In Figure 1(d), the theoretical dispersion curves are compared with the spectra as shown in Fig. 1(b) obtained by using the synthetic field.

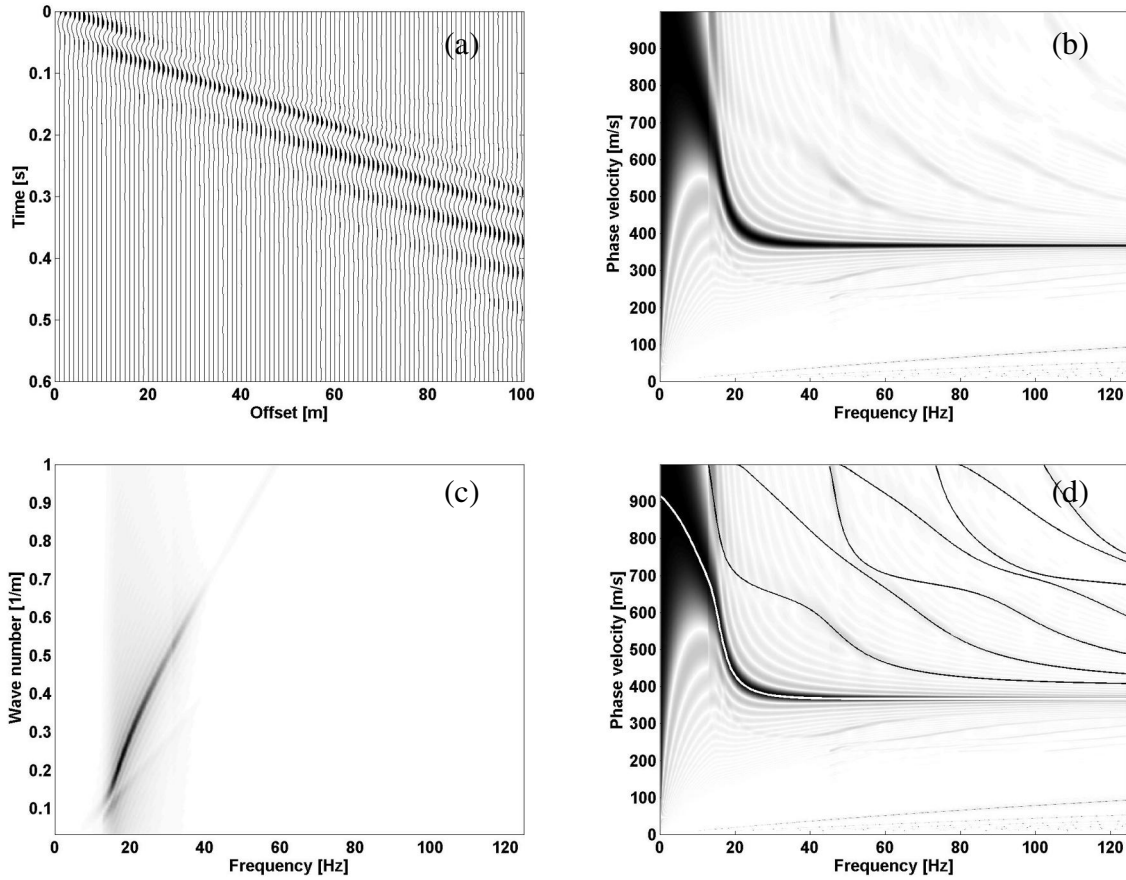


Figure 1: The dispersion analysis of the synthetic wave field, a) time history of vertical displacement, b) slant-stack analysis, c) f-k transformation and d) slant-stack transformation with the theoretical modes as eigenvalues in the used solution. Images are based on a normalized surface plot of the three-dimensional transformation results. The black values are maximum amplitudes, white values are minimum amplitudes. The dispersion branches are shown as black or dark grey areas in the upper images.

In Fig. 1(b), it is evident that the higher modes are clearly activated. Therefore, it indicates that it is not necessary to include complicated soil profiles such as wave channel or soft layers overlaid by stiffer layer to activate higher modes of surface waves. However, excitation value depends on the type and the depth of seismic source and the type of soil profile.

As can also be seen in Fig. 1(b), the resolution is poor in the low-frequency range as compared to the frequency wave number transformation (Fig.1(c)). However, when the separation of the dispersion branches in the images are of concern, the wave transformation method (Equation 2) seems to be ideal. It is also noted that a combination of different dispersion analysis methods must be used for a better image resolution, since each method has specific resolution range along the frequency axis. In the following section, the adopted procedure is used for an actual site investigation data.

## SEISMIC SITE INVESTIGATION

Several sites were investigated in the past to determine the small strain soil parameter or to determine soil profiles, so that the profiles can be compared with other methods, such as geo-electric or SCPT methods. The data presented here is from an old tailing location. The site was with deposit from mining industry activities. The deposit was approximately 30 m high covered by a sand layer on its surface. The wavefield was generated by a sledge hammer and measured using BARTEC instruments. The measured velocity seismograms were sampled with a chosen frequency of 800 Hz. The top sand cover is expected to have a higher rigidity.

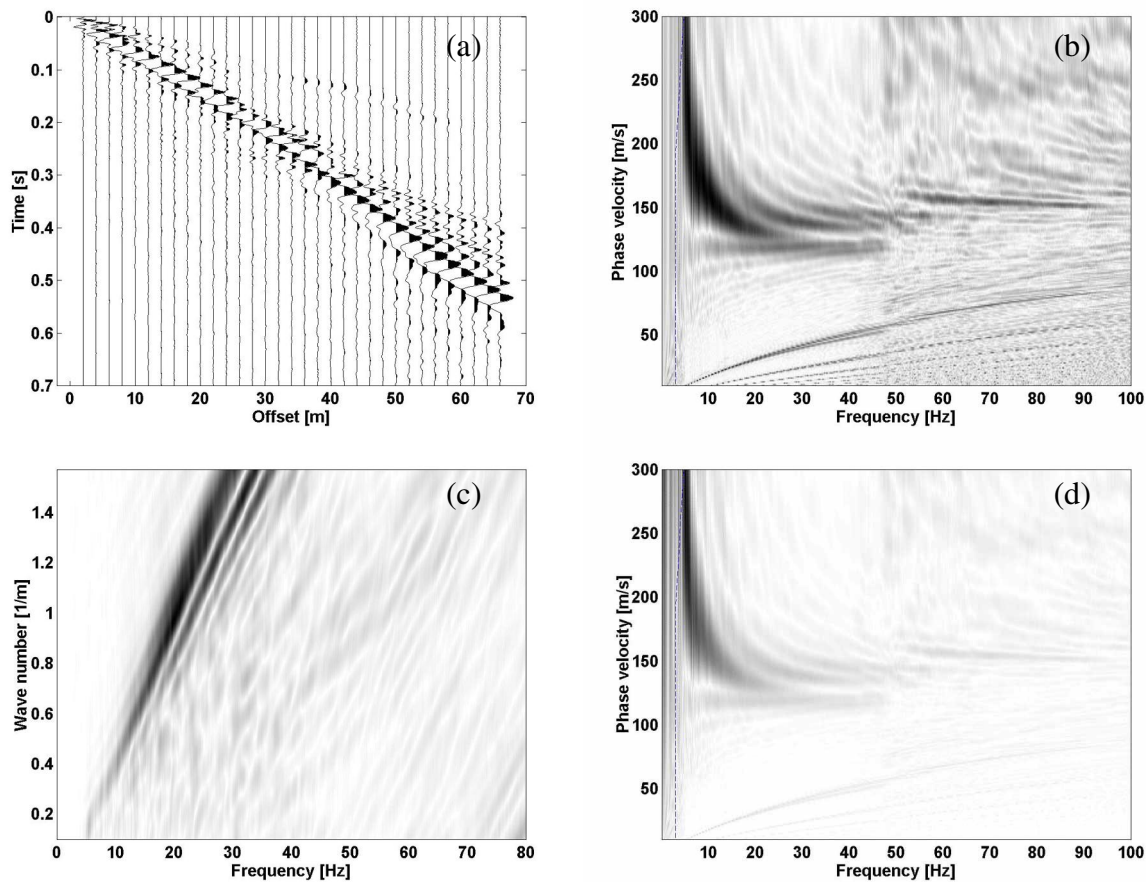


Figure 2: Dispersion analysis of the measured wave field, a) time history, b) Slant-Stack transform, c)  $f$ - $k$  transform and d) Bessel transform.

Figure 2 shows the dispersion characteristics of the site as determined based on Equations (1), (2) and (3). Furthermore, to improve the quality of the images, Equation (4) was used during the transformation of the wave field. The time history used for the offsets were from the mean value of 10 to 12 stacked shots. In this way, a better value of signal to noise ratio could be obtained as compared to considering only single shot. Fig. 2(b) and 2(d) present the result based on slant-stack transform and Bessel transform, respectively. It is evident from these figures that both the methods yield similar results. The difference between them are the amplitudes of signal and the noise level. It was also noted that if the transforms are used without the improvement as suggested by [8], it is not possible to separate the amplitudes of different modes to higher frequencies. Figure 3 shows the results without considering the improvement as suggested by [8].

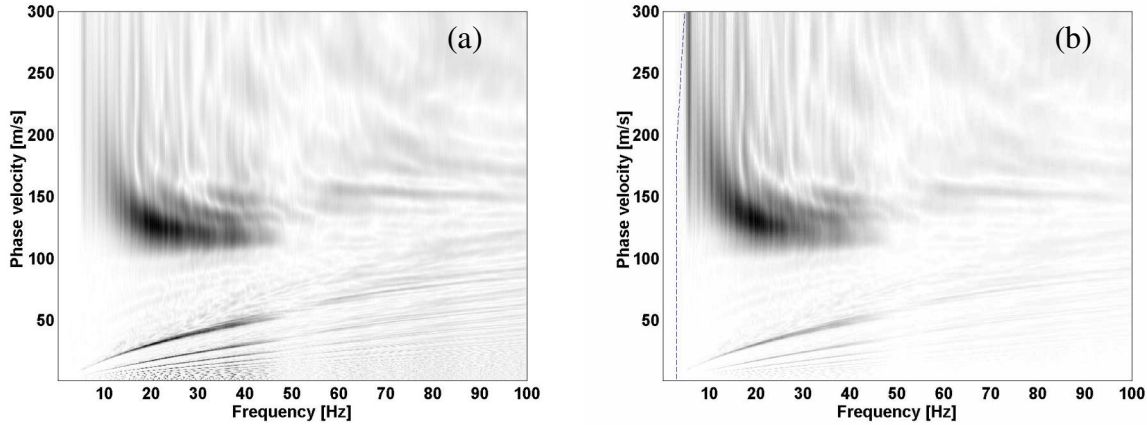


Figure 3: Dispersion analysis of the measured wave field without improvement, a) Slant-Stack transform, b) Bessel transform.

## INVERSION OF SURFACE WAVE DATA FOR DETERMINATION OF SOIL PROFILES

A least-square procedure was used as the basic inversion algorithm. For the determination of the soil profile using the measured higher modes of surface waves, the inversion procedure was modified. The non-linear dependence of the model characteristics was linearized, as is done commonly. In order to avoid the numeric instabilities of the generalized inverses during the inversion steps the Levenberg - Marquardt procedure [5] was used for the numeric stabilization. Additionally, a weighting matrix was considered, wherein the excitation of the modes from measured spectra and some values from a priori information were also considered. The objective function so obtained is:

$$\Phi(\mathbf{m}) = E + \beta L = (\delta \mathbf{d}_i - \mathbf{G}_{ij} \delta \mathbf{m}_j)^T \mathbf{W} (\delta \mathbf{d}_i - \mathbf{G}_{ij} \delta \mathbf{m}_j) + \beta (\delta \mathbf{m})^T (\delta \mathbf{m}) \quad (6)$$

With a need for the disappearing of the derivative after  $\delta \mathbf{m}^T$ , the inversion problem results in:

$$\delta \mathbf{m} = (\mathbf{G}^T \mathbf{W} \mathbf{G} + \beta \mathbf{I})^{-1} \mathbf{G}^T \mathbf{W} \delta \mathbf{d}. \quad (7)$$

In equation (7),  $\delta\mathbf{m}$  = model difference vector,  $\delta\mathbf{d}$  = data difference vector,  $\mathbf{G}$  = Jakobi matrix (matrix of the partial derivations),  $\mathbf{I}$  = unit matrix,  $\mathbf{W}$  = weighting matrix and  $\beta$  = absorption term. The bold letters in the equations describe the vector or the matrix terms.

For the application of the factorization (Singular value decomposition, SDV) in Equation (7), the weighting matrix can be decomposed as suggested by [7] into:  $\mathbf{W} = \mathbf{D}^T \mathbf{D}$  with  $\mathbf{D} = \sqrt{\mathbf{W}}$ . The weighted inversion problem results in:

$$\delta\mathbf{m} = \left( \overline{\mathbf{G}}^T \overline{\mathbf{G}} + \beta \mathbf{I} \right)^{-1} \overline{\mathbf{G}}^T \overline{\delta\mathbf{d}} \quad (8)$$

The matrices and the vectors marked by a line on the top are the weighted expressions of the original terms with the multiplication of the expressions,  $\mathbf{G}^T \mathbf{D}^T$ ,  $\mathbf{D} \mathbf{G}$  or  $\mathbf{D} \delta\mathbf{d}$ .

With the factorization  $\mathbf{G} = \mathbf{U}_p \mathbf{\Lambda}_p \mathbf{V}_p^T$  and using the term  $(\mathbf{\Lambda}_p^2 + \beta \mathbf{I})^{-1} \mathbf{\Lambda}_p$ , as suggested by [5] for embedding of the absorption term, the factorization can be indicated as:  $\mathbf{G} = \mathbf{V}_p \mathbf{K}_p \mathbf{U}_p^T$ , where  $\mathbf{V}_p$  and  $\mathbf{U}_p$  are the matrices of the eigenvectors of SVD and  $\mathbf{\Lambda}_p$  contains the positive eigenvalue,  $\lambda_i$ , from the decomposition of the Jakobi matrix,  $\mathbf{G}$ .

$$\mathbf{K}_p = \begin{bmatrix} \frac{1}{\lambda_1 + \beta/\lambda_1} & 0 & \dots & 0 \\ 0 & \frac{1}{\lambda_2 + \beta/\lambda_2} & \dots & 0 \\ \dots & \dots & \dots & \dots \\ 0 & 0 & \dots & \frac{1}{\lambda_M + \beta/\lambda_M} \end{bmatrix}$$

By considering different modes in the data difference vector,  $\delta\mathbf{d}$  can be written as:

$$\delta\mathbf{d} = \left\{ \begin{array}{c} \mathbf{d}_1 - \mathbf{d}_{1,0} \\ \mathbf{d}_2 - \mathbf{d}_{2,0} \\ \dots \\ \mathbf{d}_j - \mathbf{d}_{j,0} \end{array} \right\} \text{ with } j \in N \text{ und } j \neq 0 \quad (9)$$

where  $\mathbf{d}_j$  is the vector of the determined mode  $j$  and  $\mathbf{d}_{j,0}$  represents the corresponding mode  $j$  of the model.

If the dispersion characteristics shown in Fig. 2 were to be inverted, the separate modes have to be extracted in order to receive the information for the existing soil profile. The resulting dispersion characteristics and the shear wave profile after the inversion process was carried out and are shown in Fig. 4. In Fig. 4(a), the dispersion characteristics as obtained from the wave field transformation are also shown for comparison.

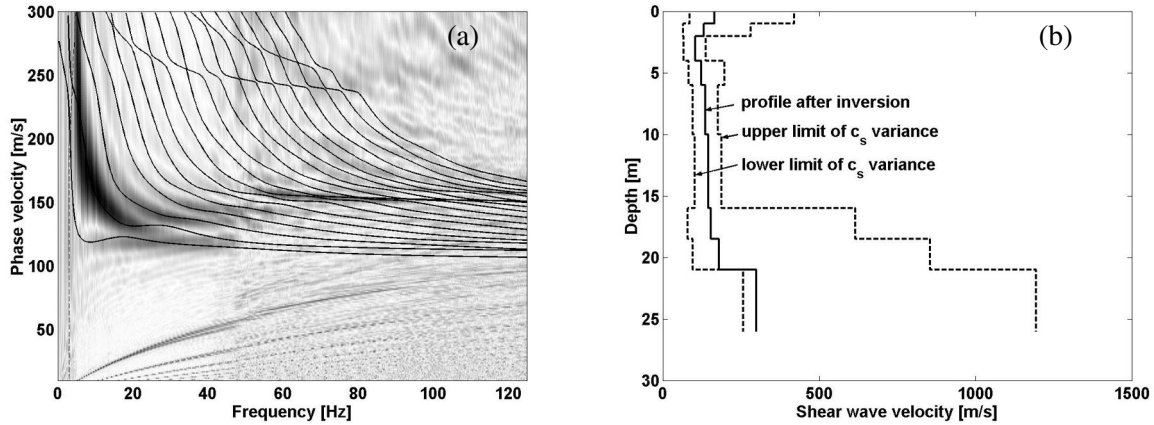


Figure 4: Results of the inverted data, a) dispersion curves of the resulting profile plotted in the measured dispersion data, b) depth-velocity profile with the variance of the shear wave velocity in each layer with a limit of 5% error.

As can be seen in Fig. 4(a), the theoretical curves take the similar form like the transformed image. The different excitation range results in different weighting factors during the inversion. The transformed image shows the expected excitation of the higher modes with increasing frequency throughout the top stiffer layer. The calculated variance of the shear wave velocity were determined by varying the partial derivations in each layer until the error limit of 5% was achieved. It gives some information about the sensibility and the validity of the inverted profile. In the range of a small variance the inverted profile possesses a greater validity. The very high variance in the deeper layer shows that no information about the shear wave velocity in the depth greater the 15 m can be obtained. The validity of the results are hence limited only to the upper 15 m depth. The reason being the absence of large wave length in the seismogram since short geophone array was used during the measurement.

A sensible point in the inversion process is the choice of initial profile of iteration. This is a property of the chosen least-square procedure during the search of the global minimum. The used search procedure is based on a linearized function while neglecting the derivatives of higher order. Therefore it is not possible to search in the whole parameter space. The initial profile has to lie at the near of the expected profile. This means that we need the knowlegde of the expected model and only a relatively small correction on the initial profile is necessary. Alternatively, in further developments the inversion procedure can be changed to a global search procedure like the grid search or genetic algorithms. But the advantage of the chosen method is a fast computation time as compared to the global search methods. Additionally, it is also possible to use subjective a priori information in the least-square procedure.

The proposed inversion method was found to work well, so far as the higher modes are separated. If there are distinct channel waves in the wave field and the separate modes become blurred to a common mode, the suggested method may not be applied. In this case the suggested method may give erroneous results in the inverted soil profile. In this case other types of inversion processes may be used.

## CONCLUSIONS

In the paper, several dispersion analysis methods were compared. It was noted that the methods are able to separate all appeared modes in the wave field. A combination of several methods seems to yield the best information about the dispersion characteristics of a given site. It is also shown that by modifying the numeric stable Levenberg - Marquardt method the inversion of higher modes of surface waves can be successfully carried out.

## ACKNOWLEDGEMENT

The authors would like to thank Dr. S.Tripathy for his valuable help during preparation of this paper.

## REFERENCES

1. Buttkus, B. "Spektralanalyse und Filtertheorie in der angewandten Geophysik." Springer Verlag, 1991.
2. Chen, X. "A systematic and efficient method of Computing Normal Modes for multilayered media." *Geophysical Journal International*, 1993, 115: 391-409.
3. Forbriger, Th. "Inversion of shallow-seismic wavefields." *Geophys. J.Int.*, 2003, 153: 719-734.
4. Hisada, Y. "An efficient method for computing Green's functions for a layered half space without sources and receivers at close depth." *BSSA*, 1994, 84(5): 1456-1472.
5. Jupp, D.L.B., Vozoff, K. "Stable iterative methods for the inversion of geophysical data." *Geophys. J. R. astr. Soc.*, 1975, 42: 957-976.
6. McMechan, G.A., Yedlin, M.J. "Analysis of dispersive waves by wave field transformation." *Geophysics*, 1981, 46(6): 869-874.
7. Menke, W. "Geophysical Data Analysis: Discrete Inverse Theory." Academic Press, 1984.
8. Park, C.B., Miller, R.D., Xia, J. "Imaging dispersion curves of surface waves in multi-channel record." (Expanded Abstract) *Soc. Explor. Geophys.*, 1998, 1377-1380.
9. Stoffa, P.L., Buhl, P., Diebold, J.B., Wenzel, F. "Direct mapping of seismic data to the domain of intercept time and ray parameter - A plane-wave decomposition." *Geophysics*, 1981, 46(2): 255-267.